



Antiproliferative activity exerted by tricyclohexylphosphane-gold(I) *n*-mercaptobenzoate against MCF-7 and A2780 cell lines: the role of p53 signaling pathways

Kok Pian Ang · Pit Foong Chan · Roslida Abd Hamid 

Received: 9 August 2020 / Accepted: 4 November 2020

© Springer Nature B.V. 2020

Abstract Based on the recent studies depicting the potential of heterometallic gold complexes as potent antiproliferative agents, herein we first reported the preliminary mechanistic data on the in-vitro antiproliferative activity of tricyclohexylphosphane-gold(I) *n*-mercaptobenzoate, $Cy_3PAu(n-MBA)$ where $n = 2$ (**1**), 3 (**2**) and 4 (**3**), and MBA = mercaptobenzoic acid, treated using MCF-7 breast cancer and A2780 ovarian cancer cells, respectively. 3-(4,5-dimethylthiazol-2-yl)-2,5-diphenyl tetrazolium bromide (MTT) assay was used to assess the cytotoxicity of both cancer cells treated with **1–3**, respectively. The IC_{50} of **1–3** were applied to the subsequent assays including cell invasion and thioredoxin reductase (TrxR) as well as ubiquitin activities specifically on Lys48 and Lys63-linked polyubiquitin chains via flowcytometric analysis. The mechanistic effect of **1–3** towards both cells were evaluated on human p53 signaling gene expressions via RT² profiler Polymerase Chain Reductase (PCR) array. **1–3** were found to be highly cytotoxic towards both MCF-7 and A2780 cancer cell lines with

the compounds were more sensitive towards the latter cells. **1–3** also suppressed TrxR and cell invasion activities by modulating p53 related genes related with proliferation, invasion and TrxR activities i.e. *CCNB1*, *TP53*, *CDK4* etc. **1–3** also regulated Lys48 and Lys63-linked polyubiquitination by reactivation of p53, suggesting the ability of this gene in regulating inhibition of cytoskeletal reorganization via epithelial–mesenchymal transition (EMT), required for tumor progression. Taken together, the overall findings denoted that **1–3** exerted potent antiproliferative activity in MCF-7 and A2780 cells via activation of the p53 signaling pathway.

Keywords p53 · Gold (I) complexes · Thioredoxin reductase · Cell invasion · Antiproliferative · MCF-7

Introduction

Concurrent global modernization leads to changes in several habits such as dietary intake, sedentary lifestyles and occupational exposure to heavy metals caused several health problems. Amongst them, cancer is one of the most major public health issues and ranked the top three leading causes of death after infectious diseases and cardiovascular diseases. Up to date, there was a total of 14.1 million new cancer cases have been reported and the mortality rate of cancer is

Electronic supplementary material The online version of this article (<https://doi.org/10.1007/s10534-020-00269-7>) contains supplementary material, which is available to authorized users.

K. P. Ang · P. F. Chan · R. A. Hamid (✉)
Department of Biomedical Science, Faculty of Medicine
and Health Sciences, Universiti Putra Malaysia,
43400 Serdang, Selangor, Malaysia
e-mail: roslida@upm.edu.my

about 9.1 million by the year 2012 (Ferlay et al. 2015). Breast cancer ranked the first reported cancer cases and cancer killer among women of all ethnic backgrounds across the world. In Malaysia, breast cancer affected status is about 1 in every 19 Malaysian women who are diagnosed by the age of 85. Approximately, 4000 women are diagnosed each year and it commonly affects the women aged between 35 to 60 and 40% of the incident rate aged below 50 years old. The risk factors of breast cancer including early menarche or late menopause, late-stage at first full-term pregnancy, high body mass index after menopause and exposure to ionizing radiation (Almutlaq et al. 2017). Simultaneously, ovarian cancer is the 5th most common cancer amongst Malaysian women. Statistically, about 500 women were diagnosed with ovarian cancer every year in Malaysia. The known risk factors of ovarian cancer including nulliparity, late menopause, early menarche, use of infertility drugs e. g. contraceptive pills and family history of breast or ovarian cancer.

Several treatment options for cancer are usually adopted and it includes radiotherapy, surgical removal, and chemotherapy, with several promising outcomes associated with various side effects (Sharma et al. 2001). However, chemotherapy that usually adopts antineoplastic drugs in killing rapid dividing cancer cells and further suppresses their proliferation is greatly utilized to increase the life expectancy of cancer patients. Most of the antineoplastic-based chemotherapy drugs are metal-based complexes and some are probably made of platinum complex employed for their anti-cancer properties. Cisplatin, the conventional antineoplastic drug of this family is one of the most widely used and the most effective cytotoxic agent in the treatment of solid tumors such as breast and ovarian cancers with the cure rate of 70–80% (Brezden et al. 2000; Donzelli et al. 2004; Taguchi et al. 2005). However, chemotherapy using cisplatin is highly limited in cancer patients due to the development of resistance by tumor cells (Boulikas and Vougiouka 2003).

It is ubiquitously known that p53 represents an attractive target for the development of anticancer therapies. It has been found most associated with human tumors of all genes, motivated drug

development efforts to (re-)activate p53 in established tumors. (Stegh 2012). It is a tumor suppressor protein that regulates the expression of a variety of genes, including apoptosis, growth inhibition, cell cycle progression inhibition, differentiation and acceleration of DNA repair, genotoxicity, and aging after cellular stress. The p53 pathway is composed of a network of genes and their products that are targeted to respond to a variety of intrinsic and extrinsic stress signals that impact upon cellular homeostatic mechanisms that monitor DNA replication, chromosome segregation and cell division (Vogelstein et al. 2000). Activation of p53 can be induced by a number of stress signals, including oxidative stress, activated oncogenes and DNA damage (Harris and Levine 2005). Whilst, the p53 protein is employed as a transcriptional activator for p53-regulated genes, resulted in cell cycle arrest, cell senescence and apoptosis (Jin and Levine 2001).

Auranofin, triethylphosphinegold(I) tetraacetylthioglucose, a gold-based anti-inflammatory compound was serendipitously discovered for its potential inhibitory activity on malignancies. The auranofin discovery enabled researchers to explore and develop more anti-cancer potential drugs utilizing gold complexes. A hypothesis was made from the presence of phosphine ligand on gold complexes which demonstrated significant cytotoxicity on cancer cells (Trudu et al. 2015; Tiekink 2002). Herein, we investigated newly synthesized auranofin analogues, tricyclohexylphosphane-gold(I) *n*-mercaptobenzoate, $Cy_3-PAu(n-MBA)$ where $n = 2$ (**1**), 3 (**2**) and 4 (**3**); MBA = mercaptobenzoic acid, to assess their antiproliferative efficacy by determining their ability to regulate cellular signaling cascades via p53-mediated signaling pathway which includes gene expression events, reorganization of cytoskeletal networks and inhibition of metastasis by preventing cancer cells invasion (Sui et al. 2015) through applying human breast adenocarcinoma cell line (MCF-7) and human ovarian carcinoma cell lines (A2780) as representative in vitro cancer cells models. This is the first report on the antiproliferative potential and its underlying mechanisms of **1–3** against cisplatin resistant cancer cells, MCF-7 and A2780 cell lines, respectively.

Materials and methods

Synthesis and characterisation

All chemicals and solvents were used as purchased without purification. All reactions were carried out under ambient conditions. Elemental analyses were performed on a Perkin Elmer PE 2400 CHN Elemental Analyser (USA). Melting points were determined on a Krüss KSP1N melting point meter (Germany). ^1H and ^{13}C NMR spectra were recorded in CDCl_3 solutions on a Bruker Avance 400 MHz NMR spectrometer (USA) with chemical shifts relative to tetramethylsilane. $^{31}\text{P}\{^1\text{H}\}$ NMR spectra were recorded in CDCl_3 solution on the same instrument but with the chemical shifts recorded relative to 85% aqueous H_3PO_4 as the external reference; abbreviations for NMR assignments: *s*, singlet; *d*, doublet; *t*, triplet; *m*, multiplet; *br*, broad. IR spectra were obtained on a Perkin Elmer Spectrum 400 FT Mid-IR/Far-IR spectrophotometer (USA) from 4000 to 400 cm^{-1} ; abbreviations: *s*, strong; *br*, broad. Powder X-ray diffraction (PXRD) data were recorded with a PANalytical Empyrean XRD system (UK) with $\text{Cu-K}\alpha 1$ radiation ($\lambda = 1.54056\text{ \AA}$) in the 2θ range 5° – 50° . The comparison between experimental and calculated (from CIF's) PXRD patterns were performed with X'Pert HighScore Plus. Stability of **1**–**3** in DMSO were tested using NMR spectroscopic method; **1**–**3** are stable up to 3 weeks with no visible changes observed from the spectra.

Synthesis of gold complexes

The preparation of **1**–**3** was similar, so that the preparation of **1** is described in detail as a representative example. The Cy_3PAuCl precursor employed in the synthesis was prepared following standard procedures by reducing KAuCl_4 (Sigma-Aldrich, USA) using one mole excess sodium sulfite (Merck, Germany), followed by addition of one mole equivalent of Cy_3P (Merck, Germany).

Preparation of $\text{Cy}_3\text{PAu}(2\text{-mba})$ (**1**)

NaOH (0.5 mmol, 0.020 g) in water (5 mL) was added to a suspension of Cy_3PAuCl (0.5 mmol, 0.256 g) in acetonitrile (20 mL), followed by addition of 2-mercaptobenzoic acid (0.5 mmol, 0.077 g) in

20 mL acetonitrile and the resulting mixture was stirred for 3 h at 50°C . The solution mixture was extracted with dichloromethane and added with equivolume of acetonitrile, which was left for slow evaporation at room temperature, yielding crystals after 2 weeks. Using the same procedures, compounds **2** and **3** were prepared and crystallised similarly.

Yield: 0.281 g (89%) colourless crystal. ^1H NMR (400 MHz, CDCl_3 , 25°C): δ 13.47 (*s*, 1H, COOH), 8.31 (*dd*, 1H, H3, $J_{\text{HH}} = 7.90, 1.66$ Hz), 7.64 (*dd*, 1H, H6, $J_{\text{HH}} = 7.78, 1.22$ Hz), 7.26 (*td*, 1H, H5, $J_{\text{HH}} = 7.49, 1.81$ Hz), 7.17 (*td*, 1H, H4, $J_{\text{HH}} = 7.56, 1.24$ Hz), 2.02–1.18 (*m*, *br*, 33H, Cy_3P) ppm. $^{13}\text{C}\{^1\text{H}\}$ NMR (400 MHz, CDCl_3 , 25°C): δ 168.2 (COOH), 139.4 (C1), 137.3 (C6), 133.0 (C3), 131.2 (C5), 131.1 (C2), 125.3 (C4), 33.2 (*d*, *i*- PC_6H_{11} , $J_{\text{CP}} = 28.20$ Hz), 30.8 (*s*, *o*- PC_6H_{11}), 27.0 (*d*, *m*- PC_6H_{11} , $J_{\text{CP}} = 12.01$ Hz), 25.8 (*s*, *p*- PC_6H_{11}) ppm. $^{31}\text{P}\{^1\text{H}\}$ NMR (400 MHz, CDCl_3 , 25°C): δ 57.8 ppm. Anal. Calc. for $\text{C}_{25}\text{H}_{38}\text{AuO}_2\text{PS}$: C, 47.62; H, 6.07. Found: C, 47.72; H, 6.22. IR: 2925 (*br*) $\nu(\text{O-H})$, 1716 (*s*) $\nu(\text{C=O})$. M.pt 174.0 – 175.0°C .

$\text{Cy}_3\text{PAu}(3\text{-mba})$ (**2**)

Yield: 0.287 g (91%) pale yellow crystal. ^1H NMR (400 MHz, CDCl_3 , 25°C): δ unobserved (1H, COOH), 8.37 (*s*, 1H, H2), 7.71 (*d*, *br*, 1H, H4, $J_{\text{HH}} = 7.80$ Hz), 7.67 (*d*, *br*, 1H, H6, $J_{\text{HH}} = 7.72$ Hz), 7.17 (*t*, 1H, H5, $J_{\text{HH}} = 7.74$ Hz), 2.11–1.24 (*m*, *br*, 33H, Cy_3P) ppm. $^{13}\text{C}\{^1\text{H}\}$ NMR (400 MHz, CDCl_3 , 25°C): δ 171.7 (COOH), 144.0 (C1), 137.2 (C6), 133.7 (C2), 128.6 (C3), 128.0 (C5), 124.8 (C4), 33.4 (*d*, *i*- PC_6H_{11} , $J_{\text{CP}} = 27.66$ Hz), 30.8 (*s*, *o*- PC_6H_{11}), 27.1 (*d*, *m*- PC_6H_{11} , $J_{\text{CP}} = 11.73$ Hz), 25.9 (*s*, *p*- PC_6H_{11}) ppm. $^{31}\text{P}\{^1\text{H}\}$ NMR (400 MHz, CDCl_3 , 25°C): δ 57.1 ppm. Anal. Calc. for $\text{C}_{25}\text{H}_{38}\text{AuO}_2\text{PS}$: C, 47.62; H, 6.07. Found: C, 47.23; H, 6.28. IR: 2925 (*br*) $\nu(\text{O-H})$, 1681 (*s*) $\nu(\text{C=O})$. M.pt 248.5 – 251.0°C .

$\text{Cy}_3\text{PAu}(4\text{-mba})$ (**3**)

Yield: 0.293 g (93%) colourless crystal. ^1H NMR (400 MHz, CDCl_3 , 25°C): δ unobserved (1H, COOH), 7.78 (*d*, *br*, 2H, H3 and H5, $J_{\text{HH}} = 8.48$ Hz), 7.61 (*d*, *br*, 2H, H2 and H6, $J_{\text{HH}} = 8.48$ Hz), 2.11–1.24 (*m*, *br*, 33H, Cy_3P) ppm. $^{13}\text{C}\{^1\text{H}\}$ NMR (400 MHz, CDCl_3 , 25°C): δ 171.0 (COOH), 153.3 (C4), 131.9 (C3), 129.6 (C2), 123.4 (C1), 33.4 (*d*, *i*- PC_6H_{11} ,

$J_{CP} = 27.64$ Hz), 30.8 (*s*, *o*-PC₆H₁₁), 27.1 (*d*, *m*-PC₆H₁₁, $J_{CP} = 11.85$ Hz), 25.9 (*s*, *p*-PC₆H₁₁) ppm. ³¹P{¹H}NMR (400 MHz, CDCl₃, 25 °C): δ 57.3 ppm. Anal. Calc. for C₂₅H₃₈AuO₂PS: C, 47.62; H, 6.07. Found: C, 47.65; H, 6.26. IR: 2924 (br) ν(O–H), 1670 (s) ν(C=O). M.pt 283.5–285.0 °C (Fig. 1).

Materials

Roswell park memorial institute medium (RPMI-1640) with high glucose, antibiotics with 10,000 U/mL penicillin and 10,000 μg/mL streptomycin, fetal bovine serum (FBS) were purchased from ScienCell Research Laboratories, USA. 0.5% Trypsin–EDTA (10 ×) was obtained from Gibco, Life Technology, UK. Matrigel™ Invasion Chamber is purchased from BD Biosciences, USA. For the solvent, ethanol (95% and absolute) was purchased from HmbG chemicals, USA and dimethyl sulfoxide (DMSO) was purchased from MERCK, Germany. All the other chemicals and reagents used in this study were of analytical grade unless otherwise stated.

Cell lines

Breast adenocarcinoma cell line, (MCF-7) was purchased from the American Type Culture Collection (ATCC), USA [ATCC catalog No.: HTB-22]. Human ovarian cancer cell line (A2780) was purchased from the European Collection of Cell Cultures (ECACC), UK [ECACC catalog No.: 93112519].

Cell culture and treatment

The MCF-7 breast cancer cells and A2780 ovarian cancer cells were cultured and maintained under standard culture conditions: 37 °C in 5% CO₂ incubator. Both cell lines were cultured in RPMI-1640 media supplemented with 10% FBS and 1% antibiotics. In this study, the trial compounds, namely Cy₃PAu(2-mba) (1), Cy₃PAu(3-mba) (2) and Cy₃PAu(4-mba) (3) respectively, associated with application of cisplatin as standard (positive) control. All compounds were dissolved in dimethyl sulfoxide (DMSO); the stock solution was prepared by dissolving the compounds in 1 mL of DMSO to obtain the stock concentration of 80 mM (80 mM).

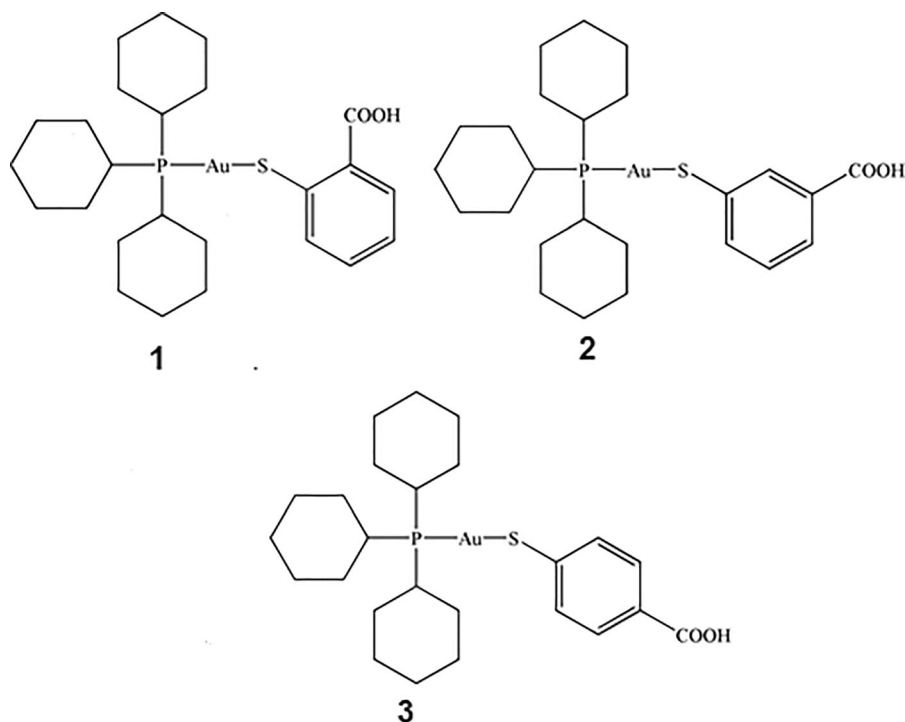


Fig. 1 Chemical structures of 1–3

Cell proliferation assay

Both MCF-7 and A2780 cancer cells were seeded at the density of 1×10^5 cells/well in 96-well plate. Compounds **1–3** were further diluted with RPMI-1640 media and added to the well (100 μ L) to obtain the final concentration of 0, 1, 5, 10, 20, 40, and 80 μ M with 0 μ M served as negative control; followed by incubation for 24 h at 37 °C in 5% CO₂ incubator. The cytotoxicity effects of **1–3** towards proliferation of MCF-7 and A2780 cells were evaluated through the MTT (3-[4,5-dimethylthiazole-2-yl]-2,5-diphenyltetrazolium bromide) assay by referring to established methods (Mosmann 1983). The MTT powder was prepared by dissolving into $1 \times$ PBS and filtered using 0.22 μ m filter to make a concentration of 2 mg/mL. The prepared MTT reagents were stored at 4 °C and covered with aluminum foil to prevent from light exposure.

After the incubation period, 20 μ L of 2 mg/mL MTT solution was added into each of the well by using multi-channel pipette. The plate was incubated again in CO₂ incubator for 2 h in dark condition. After that, the solution in the well plate was discarded by aspiration, and thereafter 100 μ L of DMSO was added into each well to dissolve the purple formazan crystal that formed at the well plate. The plate was shaken for 25 s to ensure formazan crystal had fully dissolved and homogenized. The plate was analyzed by microplate reader (BioTek EL808) at the wavelength of 570/630 nm. By using the MTT assay, the number of surviving cells after treatment of compounds **1–3** at every time interval was expressed in percentage by using the formula as below:

$$\begin{aligned} & \text{Percentage of cell viability (\%)} \\ &= \frac{\text{Absorbance of treated cells}}{\text{Absorbance of untreated cells}} \times 100 \end{aligned}$$

Graphs of various concentrations against cell viability were plotted from the calculation obtained both MCF-7 and A2780 cells, respectively. From the curves illustrated, IC₅₀ for the compounds against MCF-7 and A2780 cells were respectively obtained.

Thioredoxin reductase (TrxR) assay

MCF-7 and A2780 cells were respectively cultured at the cell density of 1×10^8 cells/well in 6-well plate and allowed for attachment overnight. Afterwards,

both types of cultured cells were treated with the respective IC₅₀ concentrations of compounds **1–3** for 24 h at 37 °C in the 5% CO₂ incubator. The cells were then harvested and collected, rinsed twice with PBS, followed by addition of 1 mL of lysis buffer consists of 10 mM Tris–HCL, 0.1 M EDTA, 5 g/mL SDS, pH 8.0 to obtain the cell lysate. The experiment was conducted according to the instruction of manufacturer protocol (Mitochondrial thioredoxin reductase assay kit, Sigma-Aldrich, USA) and lastly the activity of the enzyme was measured at 412 nm by using spectrophotometer (Thermo Scientific, USA).

Flow cytometry analysis on ubiquitin activities (Lys48-linked and Lys63-linked polyubiquitination)

The MCF-7 cells and A2780 cells were cultured in 6-well plate with the density of 1×10^6 cells/well, followed by overnight-attachment, and application of respective IC₅₀ concentrations of compounds **1–3**, with negative control received no treatment. The samples were then incubated for 24 h at 37 °C in 5% CO₂ incubator. After harvest, the cells were further washed twice with ice cold PBS to remove remnants and debris. The ubiquitin activities (Lys48-linked polyubiquitination and Lys63-linked polyubiquitination) were analyzed via flow cytometer (FACSCalibur, BD Biosciences, USA); activity of anti-ubiquitin Lys48-FITC was measured at 495 nm meanwhile activity of anti-ubiquitin Lys63-Alexa Fluor was measured at 647 nm, by following the guideline provided in manufacture's protocols (Merck-Millipore, USA).

Cell invasion assay

Cell invasion assay was carried out to investigate the inhibitory activity of compounds **1–3** towards invasion and metastasis of cancer cells, by using Matrigel™ Invasion Chamber (BD Biosciences, USA) as the in-vitro invasion model. The experiment was conducted according to the attached manufacturer's instruction. Briefly, the inserts of the invasion chamber were pre-coated with 8- μ m pore size polycarbonate membrane which give the close morphology to the endothelial cells of blood vessels, hence it was a representable model to study the inhibitory effect of compounds towards the invasion and metastasis of

cancer cells. The MCF-7 and A2780 cancer cells were seeded at the density of 1×10^5 cells in 0.5 mL of media per inserts, followed by addition of 0.5 mL of media in respective well. The cells were then treated with respective IC_{50} concentrations of **1–3** for 24 h. After the incubation period, the cells were fixed (with methanol) and stained with haematoxylin and eosin (H&E) according to the guideline and the inserts was observed under light microscope at the magnification of $\times 100$.

Human p53 signaling pathway via RT² profiler PCR array

The MCF-7 breast cancer cells and A2780 ovarian cancer cells were seeded at the density of 1×10^8 cells per 25 cm² culture flask and allowed for attachment for overnight at 37 °C in 5% CO₂ incubator. On the next day, the cells were treated with respective IC_{50} concentration of compounds **1–3** and further incubated for 24 h in standard culture condition. Prior to RNA extraction, the cells were harvested and washed twice with ice cold PBS, the samples firstly undergo DNA elimination followed by RNA extraction according to the manufacturer's instruction (DNA elimination: RNase-Free DNase Set; RNA extraction: RNeasy® Mini Kit; both from Qiagen, USA). The RNA of samples was further converted into cDNA by using the RT² first strand kit (Qiagen, USA) through the guideline provided accordingly. Lastly, the mechanistic studies on gene regulation was conducted via the RT² Profiler PCR array (Human p53 signalling pathway, PAHS-027Z). The gene expression regulated by **1–3** towards MCF-7 and A2780 cells were compared between treatment groups to negative control according to threshold level (C_t values).

Statistical analysis

Experimental data were expressed as mean \pm standard deviation (SD). Group of data were compared with one-way ANOVA with post-hoc Tukey multiple comparison test for comparison. Statistical significance was defined at $p < 0.05$.

Results

Characterization of compounds **1–3** elucidated by NMR

The compounds, Cy₃PAu(n-MBA) with n = 2 (**1**), 3 (**2**) and 4 (**3**) were prepared in high yield following the precedented procedures (de Vos et al. 1999). The crystals obtained are well soluble in chlorinated solvents and are stable against air, moisture and light. The ¹H NMR spectra of **1–3** measured in CDCl₃ showed the expected resonances attributed to n-mercaptopbenzoic acid (MBA) and tricyclohexylphosphine, which confirmed the successful coordination of the thiolate and phosphine ligands. The signals correlated to aromatic protons of –SC₆H₄COOH moiety appeared at downfield in the range of 8.37–7.17 ppm, opposed to the deshielded protons of –P(C₆H₁₁)₃ that were observed at 2.11–1.18 ppm. For **1** and **2**, four characteristic resonances were observed for aromatic protons while **3** gave rise to two pairs of broad doublets with poorly resolved coupling pattern. In the ¹H spectrum of **1**, a resonance corresponded to –COOH was identified at 13.47 ppm but the respective resonance was not observed in the case of **2** and **3**. The resonances ascribed to the respective carbon nuclei of –SC₆H₄COOH and P(C₆H₁₁)₃ were unambiguously identified in the ¹³C{¹H} spectra of **1–3**; anticipated splitting patterns were observed for carbon coupled with phosphorous. In the ³¹P NMR, a single resonance was detected at ~ 57.0 ppm, confirmed the uniformity of the compounds prepared. To evaluate the samples integrity of **1–3** in DMSO, time-dependence ¹H NMR measurements were conducted in *d*₆-DMSO and the result confirmed that **1–3** stayed intact up to at least 3 weeks with no changes observed in the ¹H spectra. The infrared spectra of **1–3** displayed the characteristic bands of $\nu(O-H)$ and $\nu(C=O)$ at approximate 2900 and 1700 cm⁻¹ respectively. Upon varying the position of –COOH at the benzene ring, a red shift to lower wavenumber was observed, i.e. 1716 cm⁻¹ to 1681 cm⁻¹ and 1670 cm⁻¹ when n = 2, 3 and 4 respectively. ESI (Suppl 1) showed that the powder X-ray patterns of **1–3** measured on bulk materials are in close agreement with the patterns calculated from the CIF files of single crystals.

Table 1 Half maximal (50%) inhibitory concentration of **1–3** towards two selected in-vitro cancer cell models: MCF-7 breast cancer cell lines, and A2780 ovarian cancer cell lines, compared with cisplatin

Compounds/cancer cell lines	MCF-7 breast cancer cells (μM)	A2780 ovarian cancer cells (μM)
1	8.14	1.19
2	7.26	2.28
3	9.03	0.785
Cisplatin	30.53	26.8

The cytotoxicity activity of **1–3** towards both cancer cell lines were measured in terms of inhibition of proliferation through the MTT viability assay. The cells were incubated for 24 h in 5% CO_2 incubator at 37 $^\circ\text{C}$, and the respective IC_{50} was calculated based on corresponding x and y values (x = concentration applied) and (y = percentage of cell viability) from the graph and data calculation software, GraphPad Prism 5.0

Cytotoxicity of compounds **1–3** towards proliferation inhibition of MCF-7 cancer cells and A2780 cancer cells

The two selected in-vitro cancer cell lines, MCF-7 and A2780 were used as representative cancers in current studies. The cytotoxicity of compounds **1–3** towards both cancer cell lines were evaluated via the MTT viability assay and the corresponding IC_{50} values were found to be 8.14, 7.26 and 9.03 μM against MCF-7 breast cancer cell lines, and 1.19, 2.28 and 0.78 μM against A2780 ovarian cancer cell lines, respectively (Table 1).

Compounds **1–3** inhibited mitochondrial thioredoxin reductase activity in MCF-7 and A2780 cancer cells

In this experiment, activity of mammalian mitochondrial thioredoxin reductase (TrxR) was analyzed by measuring the amount of 5,5'-dithiobis (nitrobenzoic acid) (DTNB) reduced by TrxR enzyme; DTNB was used as an alternative substrate of TrxR other than the NADPH. In this study, all gold compounds **1–3** exhibited inhibitory effect on thioredoxin reductase (TrxR) enzymatic activity in both MCF-7 (Fig. 2a) and A2780 (Fig. 2b) cancer cell lines. As shown in Fig. 2a, the percentage (%) of TrxR activity in MCF-7 cells treated with **1–3** was significantly attenuated to 62.70%, 52.14% and 59.70% respectively, as

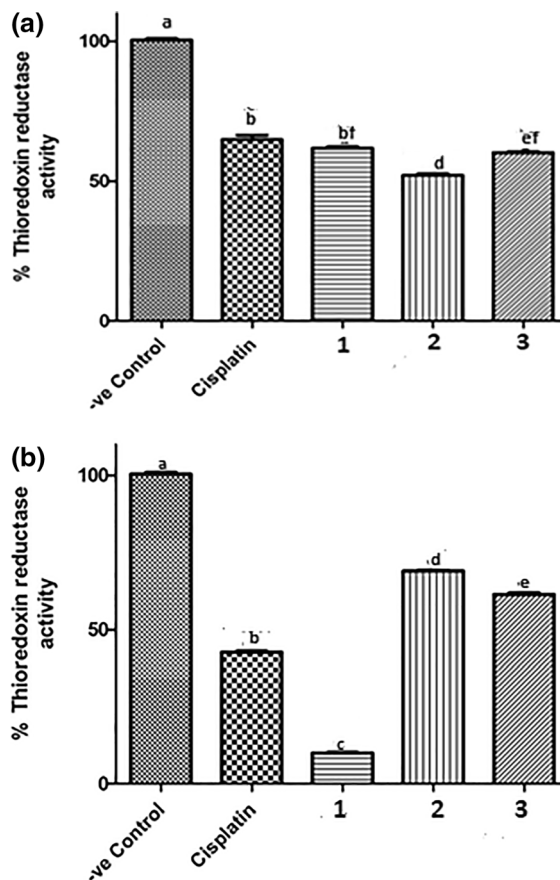


Fig. 2 The inhibitory effects of **1–3** towards mitochondrial thioredoxin reductase (TrxR) enzymatic activity of **a** MCF-7 breast cancer cell lines and **b** A2780 ovarian cancer cell lines for 24 h, respectively. Cisplatin was used as positive control. Results with different superscript letters were statistically different ($p < 0.005$)

compared to untreated cells (negative control) by assuming full enzymatic activity of TrxR. Similarly, when treated with cisplatin (standard, or positive control), TrxR activity was also suppressed to 67.63%. There was not much difference in terms of its suppression rate amongst the tested compounds, with a range from 37.3 to 40.3%. Whilst cisplatin exerted slightly lower suppression rate (32.7%) than **1–3**. In contrast, the treatment with compounds **1–3** on A2780 cancer cells also exerted similar reducing pattern in TrxR activity to 9.62%, 68.59% and 61.54%, respectively (Fig. 2b). Whilst, cisplatin that served as positive control suppressed the activity of TrxR to 42.31%. Compound **1** showed highest inhibitory rate (90.38%) on A2780 cells and showed significant

difference as compared to **2** and **3**, including the positive control cisplatin respectively.

Compounds **1–3** modulated both Lys48- and Lys63-linked polyubiquitination

The ubiquitin activities (Lys48 and Lys63) were measured via flow cytometer at 495 nm laser illuminations. Addition of anti-ubiquitin antibodies (anti-ubiquitin Lys48 and anti-ubiquitin Lys63) in the assay was also analyzed for anti-ubiquitin Lys48-FITC and anti-ubiquitin Lys63-Alexa Fluor at 647 nm. Prior to the analysis, the forward scatter and side scatter were established to exclude out cell aggregates and cell debris. The activities were represented as percentage of ubiquitin expression. Control was adjusted and calibrated to the area within 10^1 to 10^2 of the histogram, whereas untreated and treatment groups, tagged with antibodies were expressed in area M2, if they are greater than 10^2 .

Promotion of Lys48-linked polyubiquitin and suppression of Lys63-linked polyubiquitin by compounds **1–3** towards MCF-7 cancer cells were summarized in Fig. 3A(a–e). Meanwhile, results of A2780 ovarian cancer cells were summarized in Fig. 3B(a–e). As illustrated in Fig. 2A(a–e), application of IC_{50} of compounds **1–3** towards MCF-7 cancer cell lines for 24 h possessed higher Lys48-linked polyubiquitin activities and relatively lower Lys63-linked polyubiquitin activities. Exposure of MCF-7 cancer cells towards treatment resulted in increased population of detected Lys48-linked polyubiquitin (Fig. 3A(c–e)) compared to negative control (Fig. 3A(a)). Meanwhile cisplatin showed less detection of Lys48-linked polyubiquitin (Fig. 3A(b)) in contrast with treated groups. In addition, application of treatments (Fig. 3A(h–j)) including cisplatin-treated (Fig. 3(g)) exhibited lower detection of Lys63-linked polyubiquitin.

Whilst, when tested on A2780 ovarian cancer, the candidate gold compounds **1–3** exhibited similar activity as breast cancer cells, whereby higher Lys48-linked polyubiquitin activities were detected compared to Lys63-linked polyubiquitin (Fig. 3B(a–e)).

Compounds **1–3** suppressed cell invasion of MCF-7 and A2780 cells

In this study, compounds **1–3** inhibited cell invasions on MCF-7 and A2780 cancer cells, respectively. As illustrated in Fig. 4a–h, the invasion rate of MCF-7 cells treated by compounds **1–3** (Fig. 4c–e) through matrigel membrane was significantly decreased to $9.29\% \pm 0.20$, $7.41\% \pm 0.28$ and $8.45\% \pm 0.24$, respectively, compared with negative control (normalized to 100%) (Fig. 4a), whereas the positive control (cisplatin), significantly decreased cell invasion at the rate of $33.41\% \pm 1.28$, shown in Fig. 4b. There were no significant differences amongst the compounds, yet the suppression by all compounds were significantly higher than cisplatin.

Likewise, similar inhibitory pattern on A2780 was also observed when cells were treated with the gold series **1–3**, respectively as shown in Fig. 4f–j. For the treatment groups, the invasion rate of A2780 cancer cells significantly decreased by **1–3** to $36.21\% \pm 0.68$, $48.52\% \pm 2.75$ and $47.56\% \pm 1.99$ (Fig. 4h–j) respectively. The positive control (cisplatin) exhibited the cell invasion rate at $42.15\% \pm 2.13$, (Fig. 4g) which gave almost similar efficacy as **2** and **3**, but not **1**. All treatment groups in both cancer cells, MCF-7 and A2780 cancer cells significantly suppressed the cell invasion rate as compared to negative control (normalized to 100%, respectively ($p < 0.005$)). The graphical results of cancer cells invasion studies were summarized in Fig. 4k (for MCF-7 breast cancer cells) and Fig. 4l (for A2780 ovarian cancer cells).

Compounds **1–3** regulated p53 related gene expression in MCF-7 and A2780 cells

In order to analyze the ability of compounds **1–3** to regulate the most common cellular signaling cascade in both selected cancer cells, the human p53 signaling pathway, consists of the key components of downstream targeted genes involved in cell proliferation and cell cycle, apoptosis, organization of cytoskeletal networks as well as cellular migration and metastasis. However, in this study, we just focused on the related genes which involved in the activities studied which are cell proliferation, TRxR and ubiquitin activities as well as cell invasion. Herein, treatment of compounds **1–3** towards MCF-7 cells (Table 2) induced

Fig. 3 **A** Histograms depicting MCF-7 cells stained using the anti-ubiquitin Lys-48 specific, FITC conjugate and antiubiquitin Lys-63 specific, Alexa Fluor® 647 conjugate upon treatment with (a) negative control (untreated cells), corresponding IC₅₀ values of (b) cisplatin; (c) **1**, (d) **2**, and (e) **3** for 24 h. **B** Histograms depicting A2780 cells stained using the anti-ubiquitin Lys-48 specific, FITC conjugate and antiubiquitin Lys-63 specific, Alexa Fluor® 647 conjugate upon treatment with (a) negative control (untreated cells), corresponding IC₅₀ values of (b) cisplatin; (c) **1**, (d) **2**, and (e) **3** for 24 h

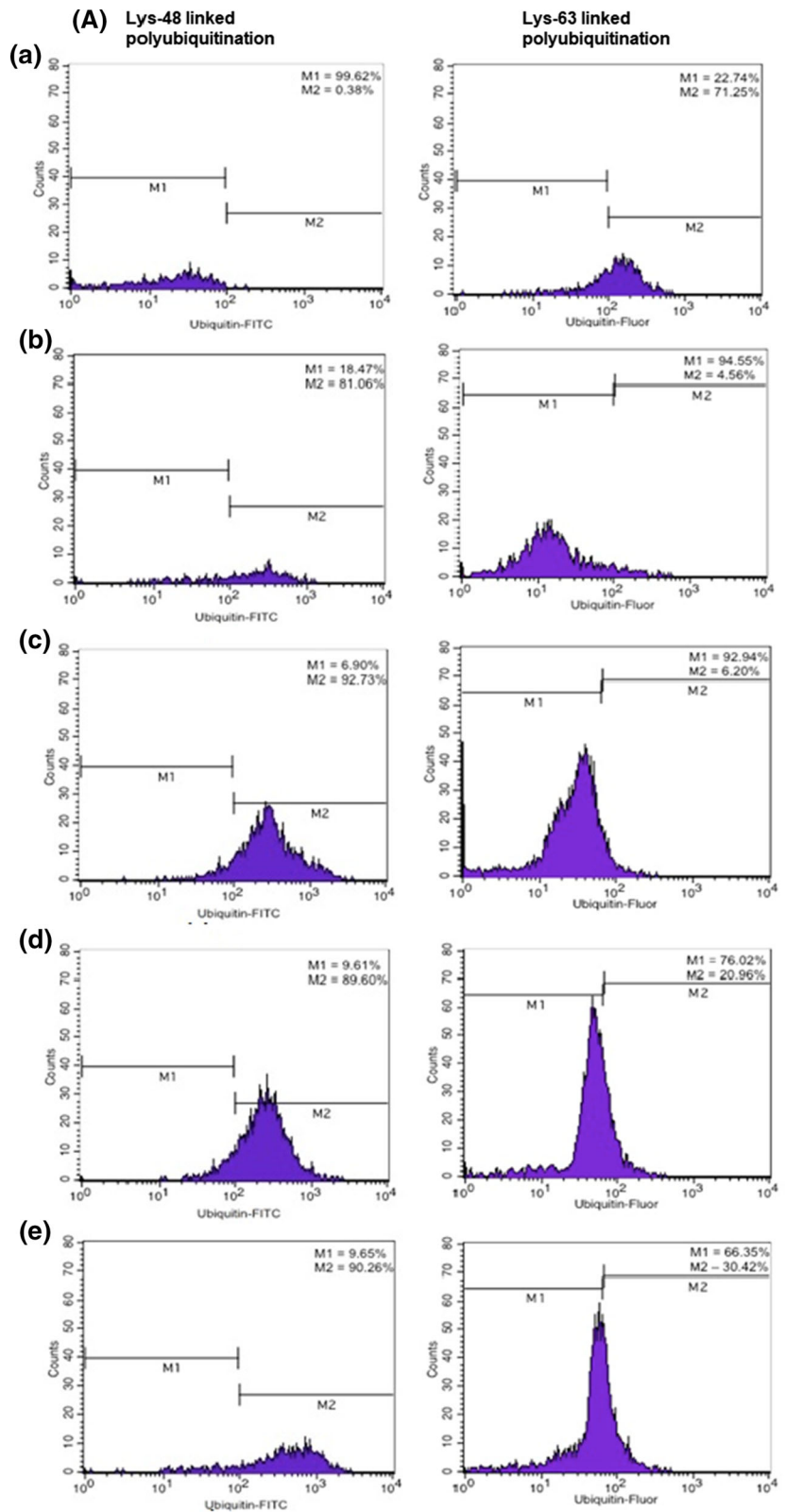
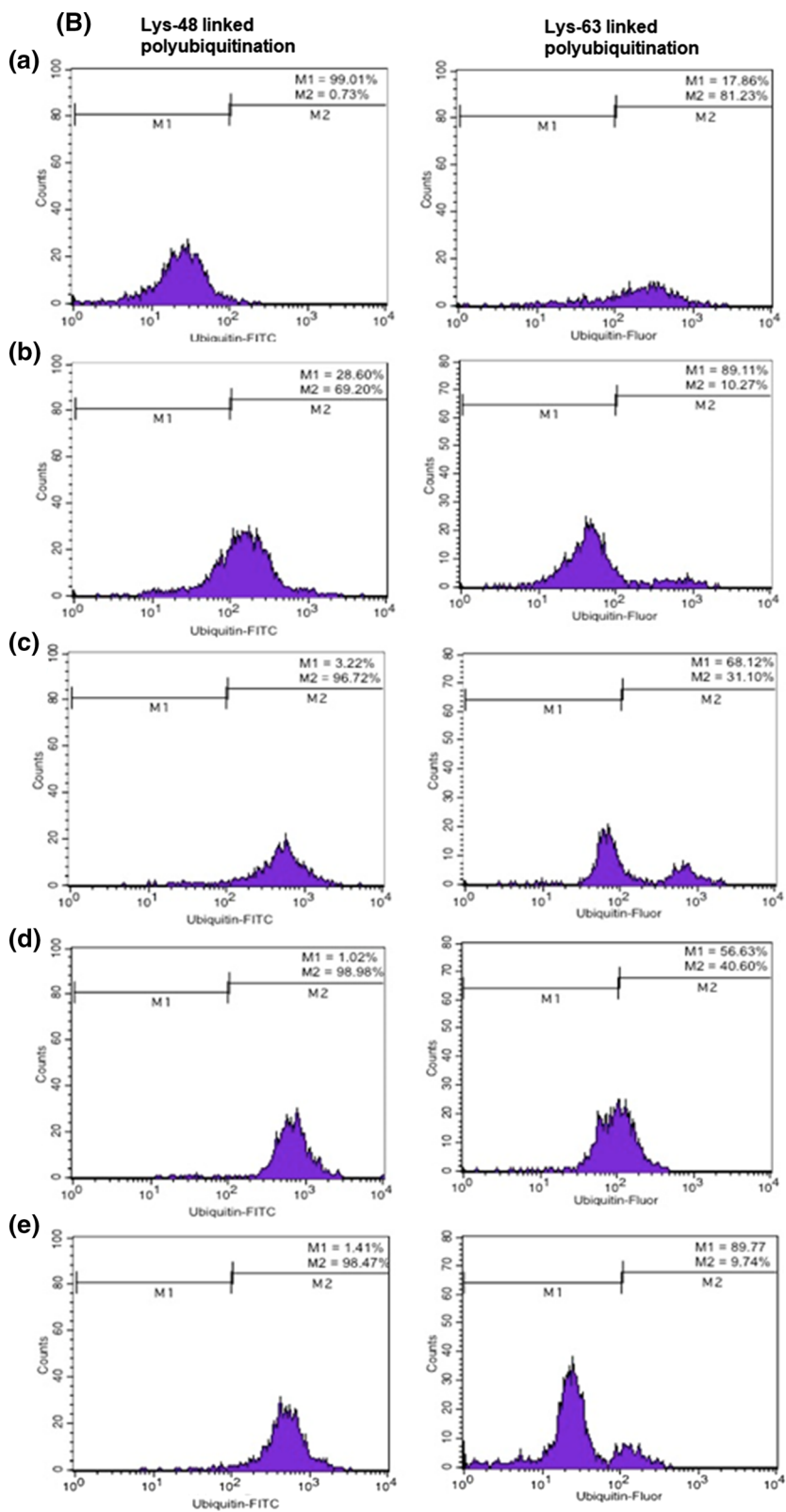


Fig. 3 continued



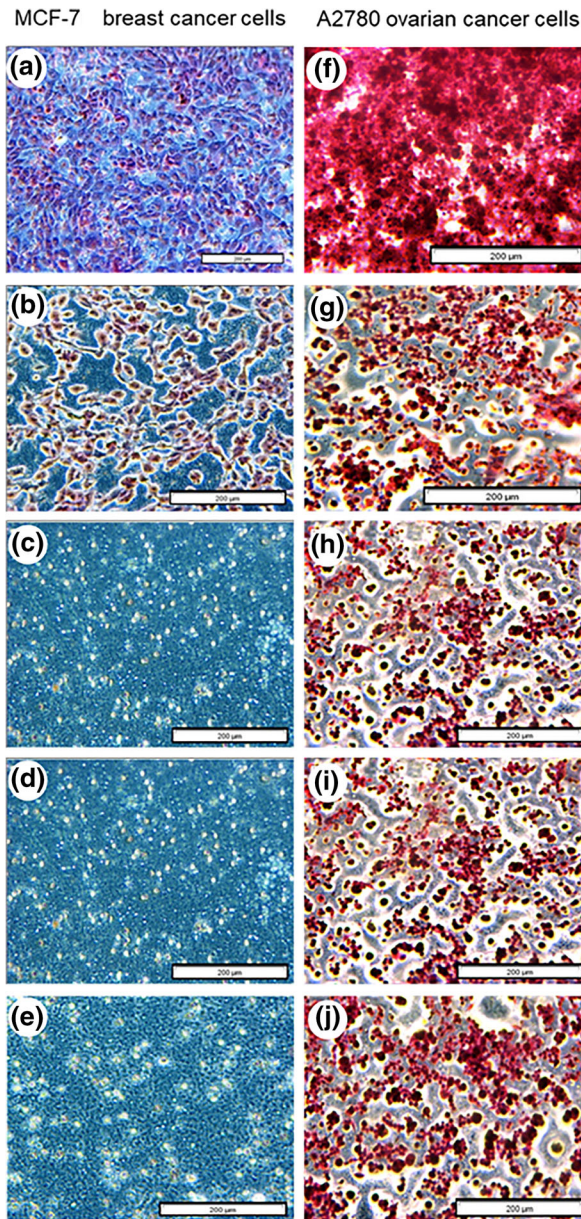
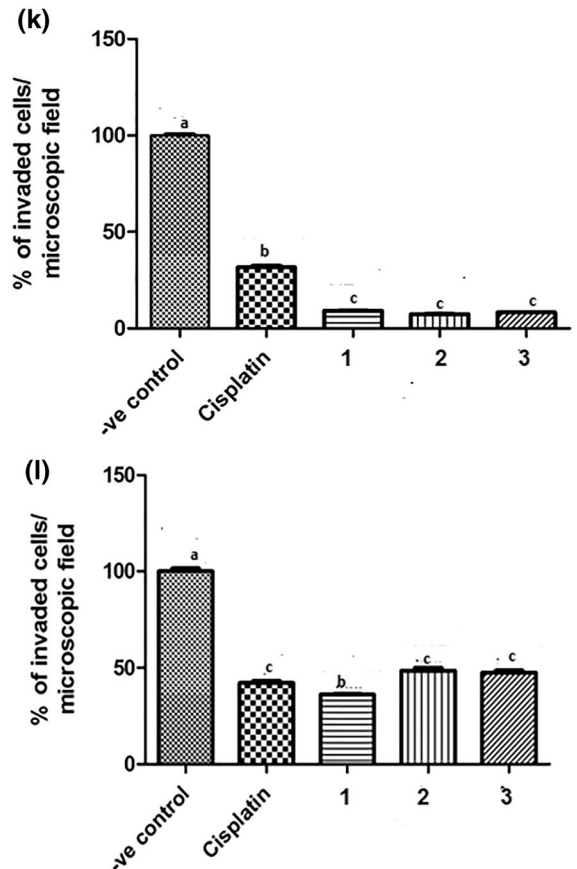


Fig. 4 Qualitative findings of cell invasion assay illustrated by 1–3 towards MCF-7 breast cancer cells, with **a** negative control, **b** cisplatin, **c** 1, **d** 2, and **e** 3; followed by A2780 ovarian cancer cells, with **f** negative control, **g** cisplatin, **h** 1, **i** 2, and **j** 3; The graphical results of cell invasion were further amended in **k** MCF-7 breast cancer cells and **l** A2780 ovarian cancer cells.

expression of extrinsic apoptosis pathway genes together with its upstream regulator, up-regulation of TNF gene and down-regulation of FAS gene families. Furthermore, many other important genes associated with extrinsic apoptosis and p53 signal transduction



Results were mean of three independent experiment (n = 3); each microscopic image is representative from ten random microscopic field from the same Matrigel invasion chamber, and the number of cells were calculated by using the cell counter. [Magnification: × 100]. Data with different superscript letters were significantly different, ($p < 0.005$)

pathway was also found to be modulated (up-regulated and down-regulated) upon treatment with compounds 1–3.

As 1–3 have shown high antiproliferative activities towards MCF-7 cells, related tumor suppressor genes

Table 2 p53 related gene expression level upon treatment with 1–3 towards MCF-7 breast cancer cells, compared to the negative control group

Gene	Up/Down Regulation Fold Regulation (compared to control group)		
	1	2	3
APAF1	8.39	5.37	13.92
ATM	20594.90	578.52	-11.23
ATR	306.55	-1.00	-51.62
BAI1	1.52	-1.05	-127.11
BAX	50.21	86.59	10.70
BBC3	38.31	1.05	-1.70
BCL2	-11.63	-23.16	-32.89
BCL2A1	-6.63	-1.67	-1.70
BID	404.50	2346.42	46.52
BIRC5	-83.28	-3.34	-6.63
BRCA1	2.62	-1.04	4.72
BRCA2	26.35	2.05	3.29
BTG2	-1.07	1.04	-4.78
CASP2	9.57	3.47	69.07
CASP9	4.28	57.13	326.28
CCNB1	-82.14	-84.67	-2.97
CCNE1	30.91	1717.67	2896.31
CCNG1	-9.78	-78.45	-2.16
CCNH	-1.23	-5.67	-3.76
CDC25A	-22.78	-7.38	-22.01
CDC25C	-3.41	-3.66	-12.73
CDK1	-15.03	-2.92	-79.34
CDK4	-46.53	-2.27	-259.57
CDKN1A	2.28	1.76	187.40
CDKN2A	5.54	5428.13	8841.04
CHEK1	1.53	-4.70	-1.06
CHEK2	1.69	-1.03	-2.91
CRADD	39.40	13.42	23.75
DNMT1	-3.29	-21.46	-32.00
E2F1	2.41	7.71	7.41
E2F3	10.56	-1.57	-1.13
EGFR	-7.11	-12.59	-1.72
EGR1	6.63	2.86	1.12
EL24	-2.13	-16.38	-27.10
ESR1	-1.45	-6.74	-16.68
FADD	-19.43	-126.57	-30.06
FAS	-15.03	-52.48	-11.24
FASLG	-1.43	-2.16	-7.62
FOXO3	-1.22	-9.74	-30.27
GADD45A	-2.22	-4.90	-7.01
GML	347.29	-17.43	-61.82
HDAC1	-1.06	-4.70	-5.70
HK2	2.62	-2.12	-2.33
IGF1R	1.39	-4.36	-7.46
IL6	-2.89	-1.67	-97.01
JUN	-3.07	-1.76	-76.64
KAT2B	-4.72	-9.81	-5.58
KRAS	3.34	109.61	724.08
MCL1	-1.82	-5.22	-10.56
MDM2	-2.27	-4.30	-23.10
MDM4	1.18	-61.55	-106.15
MLH1	-2.46	-3.56	-40.79
MSH2	-1.21	-6.21	-10.48
MYC	1.17	-2.82	-4.50
MYOD1	60.97	13.61	-1.58
NF1	-1.24	-1.56	-16.11
NFKB1	-64.45	-585.60	-73.52
PCNA	-10.78	-43.83	-714.11
PIDD	-5.17	-14.66	-177.29
PPM1D	45.57	-1.14	-14.72
PRC1	2.07	-1.15	-5.90
PRKCA	652.58	-2.96	4.92
PTEN	-3.48	-22.84	-15.56
PTTG1	-2.19	-2.27	-98.36
RB1	-1.80	-5.18	-19.84
RELA	-1.56	-6.52	-18.51
PRPM	33.82	-6.65	321.79
SESN2	1.43	-2.17	-4.02
SLAH1	891.44	-16.26	24.25
SIRT1	2.49	1.26	-2.58
STAT1	1.98	-2.91	-1.31
TADA3	-1.65	-5.79	-14.82
TNF	3.65	8.49	5.93
TNFRSF10B	6.72	1.78	1.31
TNFRSF10D	2.51	-1.27	-1.39
TP53	8.00	2.33	6.45
TP53AIP1	349.70	3.40	765.36
TP53BP2	103.25	12.61	2.01
TP63	-1.48	-2.31	-3.34
TP73	274.37	223.82	1351.17
TRAF2	248.99	3.96	5.73
TSCI	12.04	-3.43	2.37
WT1	-132901.60	-14342168.63	-2336.28
XRCC5	-1.29	-6.20	-10.41

Data represent means of samples 1–3 induced fold-change in gene expression, relative to control treated cells. ($n = 3$) $p < 0.05$. Red, up-regulated genes; blue, down-regulated genes and plain text, no detectable change

directly/indirectly involved in MCF-7 cell proliferation were shown to be upregulated by **1–3** which are p21 encoded genes, *CDKN1A* (28-, 1874.2-fold), *CDKN2A* (5.54-, 5428.13 and 8841.04- fold). In addition **1** and **2** also significantly upregulated *ATM* by 20,594.90- and 578.52-fold, respectively. Whilst, **1–3** also downregulated *CDK4* (– 46.63, – 2.27 and – 259.57 fold), *CDK1* (– 15.03, – 2.92 and – 79.34 fold), *CCNBI* (– 82.14, – 84.07 and – 2.97 fold), *CCNG1* (– 9.78, – 78.45 and – 2.16 fold) *CDC25A* (– 22.78, – 7.38 and – 22.01 fold), *PCNA* (– 10.78, – 43.83 and – 714.11 fold), *CDC25C* (– 3.41, – 3.66 and – 12.73 fold), *WT1* (– 132,901.60, – 14,342,168.63 and – 2336.28 fold), respectively. Whilst, *MYC*, *IGF1R* and *ESR1* were only downregulated by **2** and **3** by (– 2.82, – 4.50 fold), (– 4.36, – 7.46 fold) and (– 6.74, – 16.68 fold), respectively.

On the other hand, it has been reported that TrxR inhibitory directly modulated the cell cycle arrests as well as apoptosis. Hence, there is a direct correlation between TrxR activity with the modulation of cell cycle and apoptotic-related genes (Selenius et al. 2012). This activity was significantly suppressed by **1–3** and this was confirmed by modulation of several genes directly/indirectly related with the TrxR suppression/inhibition i.e. *BCL2* (– 11.63, – 23.16 and – 32.89-fold), *BID* (404.50-, 2346.42- and 46.52-fold), *CCNBI* (– 82.14, – 84.67 and – 2.97-fold), *CDK4* (– 46.53, – 2.27 and – 259.57-fold), *MDM2* (– 2.27, – 4.30, and – 23.10-fold) respectively. Meanwhile, *ESR1* was only modulated by **2** and **3** by – 6.74 and – 16.68-fold; *PRCI* by **1** only (– 5.90-fold).

Notwithstanding, all compounds were also shown to suppress MCF-7 cancer cells invasion and this has been confirmed with the downregulation of several genes related with invasion i.e. *BIRC5* (– 83.28, – 3.34 and – 6.63-fold), *CDK4* (– 46.53, – 2.27 and – 259.57 fold), *PCNA* (– 10.78, – 43.83, – 714.11-fold), *NFKB1* (– 64.45, – 585.60 and – 73.52-fold), respectively. Whilst, *CCNH* (– 5.67, – 3.76-fold), *MYC* (– 2.82, – 4.50-fold), *RELA* (– 6.52 and – 18.51-fold) and *TP63* (– 2.31 and – 3.34-fold) were significantly downregulated by **2** and **3**; *JUN* by **1** and **3** (– 3.07 and – 76.64-fold); *EGFR* by **1** and **2** (– 7.11, – 12.59 fold); *PRKCA* by **1** (– 2.96-fold); *STAT1* by **2** (– 2.91 fold), respectively. On the other

hand, *BAX* (50.21-, 86.59- and 10.70-fold), *BID* (404.50-, 2346.42- and 46.52-fold), *CCNE1* (30.91-, 1717.67-, 2896.31- fold), *E2F1* (2.41-, 7.71- and 7.41-fold), *APAF-1* (8.39-, 5.37- and 13.92-fold), *KRAS* (3.34-, 109.61-, 724.08-fold), *TP53* (8-, 2.33 and 6.45-fold), *TP53AIP1* (349.70-, 3.40- and 765.36-fold), *TP53BP2* (103.25-, 12.61- and 2.01-fold), *TP73* (274.37-, 223.83- and 1351.17-fold), *TNF* (3.65-, 8.49- and 5.93-fold), *TRAF-2* (249-, 3.96- and 5.74-fold) were significantly upregulated by **1–3**, and *TSC1* by **1** and **3** (12.04- and 2.37-fold), respectively.

Table 3 shows the p53 mediated gene expression data on A2780 ovarian cells treated with **1–3**, respectively. **1–3** also exhibited high antiproliferative, TrxR inhibition and anti-invasive activities which are confirmed by the downregulation of several related oncogenes as follows; *BCL2* (– 57.68, – 3.78 and – 10.41-fold), *BCL2AI* (– 11.19, – 2.22 and – 9.00-fold), *BIRC5* (– 4.99, – 34.49 and – 10.27-fold), *BRCA1* (– 4.72, – 2.62 and – 18.10-fold), *BRCA2* (– 2.85, – 4.11 and – 2.04-fold), *CCNBI* (– 22.63, – 10.56 and – 7.11-fold), *CCNH* (– 3.48, – 15.65 and – 6.41-fold), *CDC25A* (– 17.98, – 13.70 and – 17.49-fold), *CDC25C* (– 67.65, – 40.12 and – 50.21-fold), *CHEK1* (– 69.07, – 5.86 and – 37.27-fold), *CHEK2* (– 5.78, – 2.95 and – 5.86-fold), *EGFR* (– 60.89, – 19.11 and – 22.29-fold), *GML* (– 18.20, – 17.39 and – 8.46-fold), *HK2* (– 25.96, – 3.86 and – 89.26-fold), *NFKB1* (– 23.10, – 4.44 and – 15.67-fold), *MDM4* (– 5.66, – 5.13 and – 5.17-fold), *RELA* (– 10.63, – 3.56 and – 6.50-fold) and *TP63* (– 11.46, – 11.54 and – 8.62-fold), respectively. Whilst, compounds **1** and **3** were shown to down-regulate *CDK1* (– 2.14 and – 4.23-fold), *CDK4* (– 3.92 and – 6.28-fold) and *MDM2* (– 2.51 and – 3.07-fold), respectively.

On the contrary, **1–3** significantly upregulated *APAF1* (3.73-, 62.25- and 35.26-fold), *CASP9* (28.44-, 5.94- and 53.82-fold), *CDKN1A* (14.20-, 2.00- and 13.91-fold), *FAS* (29.45-, 17.10- and 18.00-fold), *FASLG* (66.72-, 6.65- and 2.16-fold), *JUN* (3.29-, 8.75- and 4.69-fold), *KRAS* (8.49-, 2.69- and 25.81-fold), *RBI* (41.36-, 2.03- and 55.72-fold), *TP53* (4.32-, 57.68- and 11.79-fold), *TP53AIP1* (3.78-, 6.09- and 5.84-fold), *TP53BP2* (5.89-, 2.17- and 6.58-fold), *TP73* (3.20-, 8.39- and 6.96-fold) and *TSC1* (5.46-, 4.74- and 8.57-fold), respectively. In addition,

Table 3 p53 dependent gene expression level upon treatment with 1–3 towards A2780 ovarian cancer cells, compared to the negative control group

Gene	Up/Down Regulation Fold Regulation (compared to untreated control)		
	1	2	3
<i>APAF1</i>	3.73	62.25	35.26
<i>ATM</i>	20.39	-1.05	33.36
<i>ATR</i>	5.21	-3.71	58.49
<i>BAI1</i>	-65.80	-1.51	-35.75
<i>BAX</i>	10.34	1.72	28.25
<i>BBC3</i>	-1.45	22.94	-1.51
<i>BCL2</i>	-57.68	-3.78	-10.41
<i>BCL2A1</i>	-11.19	-2.22	-9.00
<i>BID</i>	41.36	1.78	29.45
<i>BIRC5</i>	-4.99	-34.49	-10.27
<i>BRCA1</i>	-4.72	-2.62	-18.10
<i>BRCA2</i>	-2.85	-4.11	-2.04
<i>BTG2</i>	-7.57	12.82	-2.97
<i>CASP2</i>	1.56	2.13	2.35
<i>CASP9</i>	28.44	5.94	53.82
<i>CCNB1</i>	-22.63	-10.56	-7.11
<i>CCNE1</i>	-5.39	-1.04	-3.01
<i>CCNG1</i>	-1.73	-27.86	-1.07
<i>CCNH</i>	-3.48	-15.65	-6.41
<i>CDC25A</i>	-17.98	-13.70	-17.49
<i>CDC25C</i>	-67.65	-40.12	-50.21
<i>CDK1</i>	-2.14	-4.23	-1.75
<i>CDK4</i>	-3.92	-6.28	-1.30
<i>CDKN1A</i>	14.20	2.00	13.91
<i>CDKN2A</i>	-1.01	-1.62	-1.21
<i>CHEK1</i>	-69.07	-5.86	-37.27
<i>CHEK2</i>	-5.78	-2.95	-5.86
<i>CRADD</i>	-23.26	-7.26	-6.36
<i>DNMT1</i>	14.03	11.54	25.28
<i>E2F1</i>	9.32	45.76	8.11
<i>E2F3</i>	14.83	2.53	2.89
<i>EGFR</i>	-60.89	-19.11	-22.29
<i>EGR1</i>	-3.29	2.87	-2.64
<i>EL24</i>	-2.23	-5.96	-1.41
<i>ESR1</i>	-3.05	2.98	-1.14
<i>FADD</i>	13.74	8.75	10.06
<i>FAS</i>	29.45	17.10	18.00
<i>FASLG</i>	66.72	6.65	2.16
<i>FOXO3</i>	12.55	-12.38	14.93
<i>GADD45A</i>	-4.66	-1.27	-1.92
<i>GML</i>	-18.20	-17.39	-8.46
<i>HDAC1</i>	16.45	58.89	29.04
<i>HK2</i>	-25.96	-3.86	-89.26
<i>IGF1R</i>	4.17	1.10	4.03
<i>IL6</i>	-4.13	-17.01	-3.33
<i>JUN</i>	3.29	8.75	4.69
<i>KAT2B</i>	1.77	5.28	4.69
<i>KRAS</i>	8.49	2.69	25.81
<i>MCL1</i>	3.16	-23.10	-1.80
<i>MDM2</i>	-2.51	-3.07	-1.38
<i>MDM4</i>	-5.66	-5.13	-5.17
<i>MLH1</i>	-4.25	-4.12	-6.13
<i>MSH2</i>	-1.32	53.45	1.17
<i>MYC</i>	1.79	-4.16	1.61
<i>MYOD1</i>	8.10	16.56	1.05
<i>NF1</i>	-2.60	22.94	-1.06
<i>NFKB1</i>	-23.10	-4.44	-15.67
<i>PCNA</i>	-1.74	-14.52	-1.54
<i>PI3K</i>	-13.07	-38.48	-71.01
<i>PPM1D</i>	-5.43	3.16	-3.01
<i>PRC1</i>	-1.22	17.63	1.62
<i>PRKCA</i>	-54.57	-68.12	-26.72
<i>PTEN</i>	1.66	16.34	5.58
<i>PTTG1</i>	-2.25	-9.88	-3.27
<i>RB1</i>	41.36	2.03	55.72
<i>RELA</i>	-10.63	-3.56	-6.50
<i>PRPM</i>	-8.49	-7.15	-6.63
<i>SESN2</i>	-4.89	9.99	-5.28
<i>SLAH1</i>	-45.89	-12.19	-4.59
<i>SIRT1</i>	-2.68	-47.50	-1.93
<i>STAT1</i>	-2.30	-2.48	-1.03
<i>TADA3</i>	3.29	-5.39	4.43
<i>TNF</i>	-72.00	-16.00	-17.36
<i>TNFRSF10B</i>	-2.46	2.60	-3.51
<i>TNFRSF10D</i>	-85.04	-9.38	-55.33
<i>TP53</i>	4.32	57.68	11.79
<i>TP53AIP1</i>	3.78	6.09	5.84
<i>TP53BP2</i>	5.89	2.17	6.58
<i>TP63</i>	-11.46	-11.54	-8.62
<i>TP73</i>	3.20	8.39	6.96
<i>TRAF2</i>	29.45	-1.62	43.11
<i>TSCI</i>	5.46	4.74	8.57
<i>WT1</i>	-11.60	3.71	-9.96
<i>XRCC5</i>	1.95	1.78	2.04

Data represent means of samples 1–3 induced fold-change in gene expression, relative to control treated cells. ($n = 3$) $p < 0.05$. Red, up-regulated genes; blue, down-regulated genes and plain text, no detectable changes

BAX (10.34-, and 28.25-fold), *BID* (41.36- and 29.45-fold), *FOXO3* (12.55- and 14.93- fold) and *TRAF2* (29.45- and 43.11- fold) were only up-regulated by **1** and **3** by and respectively. Whilst, *PTEN* (16.34- and 5.58-fold) and *CASP2* (2.13- and 2.35-fold) were significantly upregulated by **2** and **3**; *SESN2* (9.99-fold) by **2** only.

Discussion

The synthesized gold(1) complex with bis-ligand i.e. tricyclohexyl and *n*-mercaptobenzoic acid (*n*-MBA) i.e. 2-MBA, 3-MBA and 4-MBA were successfully synthesized. Initially, the phosphane-gold(1) complexes have been characterized by Tiekink and workers in the mid-90 s and early 2000s (de Vos et al. 1999,2002) and their compounds' crystallization have also been characterized previously (de Vos et al. 2002; Cookson and Tiekink 1992; Smyth et al. 2001).

In this current study, confirmation of the chemical structures of **1–3** was characterized by ^1H , ^{13}C and ^{31}P NMR spectra, respectively via both CDCl_3 and $\text{d}_6\text{-DMSO}$ solution as exhibited in the previous study by Cookson and Tiekink (Cookson and Tiekink 1992). They have reported elucidation of the compounds' structures via ^1H and ^{13}C NMR obtained in $\text{d}_6\text{-DMSO}$ solution were similar to those obtained in chlorinated solvents suggesting no interaction between the complex and the solvent. Ultimately, ^{31}P NMR spectra of the compound was shown to possess similar chemical shifts in both CDCl_3 and $\text{d}_6\text{-DMSO}$, in which these resonances are in the range expected for complexes of this type (Cookson and Tiekink 1992), which justified the implication of ^{31}P NMR to characterize **1–3** in this current study.

Additionally, DMSO was used to dissolve the compounds in the biochemical/molecular studies. Besides, DMF was also been used a stock solution for gold(1) complexes of water soluble diphos-type ligand in TrxR activities (Wetzel et al. 2011). Elie et al. (2009) reported the use of PBS (NaCl 0.9%) to dissolve the water soluble phosphane-gold(1) complexes to determine their cytotoxicities against Jurkat cells. Other than that, PBS can also be used to dissolve water-soluble gold(1) phosphine complexes such as sulfonated arylphosphines (abbreviated TPPMS, TPPDS, TPPTS), 1,3,5- triaza-7-phosphaadamantane (TPA) (Daigle et al. 1974) or 3,7-diacetyl-1,3,7-

triaz-5-phosphabicyclo[3.3.1]nonane (DAPTA) (Darensbourg et al. 2004).

It has been reported that phosphine-gold(1) thiolates were more cytotoxic than gold(I) thiolates, and that phosphine-gold(I) thiolates had more promising cytotoxicity profiles than their chloride analogues, indicating the importance of both the phosphine and the thiolate ligand for cytotoxic activity (Gandin et al. 2010). Therefore, here in we reported the cytotoxic potential of phosphane-gold(1) thiolate derivatives; tricyclohexylphosphane-gold(I) *n*-mercaptobenzoate, $\text{Cy}_3\text{PAu}(n\text{-mba})$ where $n = 2$ (**1**), 3 (**2**) and 4 (**3**), against MCF-7 breast cancer cells and A2780 ovarian cancer cells in order to understand their potential as antiproliferative agent. Compounds **1–3** have been shown to suppress the cell proliferation of cisplatin sensitive cells lines, MCF-7 and A2780 cell lines, respectively with low IC_{50} values in low μM range. In a similar study by deVos et al. (2002), the similar phosphane-gold (1) complexes have also been previously tested for their IC_{50} using Sulfurhodamine B (SRB) assay towards MCF-7 cells, which reported lower range of ID_{50} values (411–973 ng/mL) and comparable to cisplatin compared to the our current findings. In addition, triethylphosphane-gold(1)-*n*-MBA and triphenylphosphane-gold(1)-*n*-MBA were also tested by the same authors and were shown to exert higher ID_{50} compared to the former complexes (de Vos et al. 2002). In another study by de Vos et al. (2004), the cytotoxicity of tricyclohexylphosphane-gold (1) with dithiocarbamates and xanthates as ligands were determined which yielded lower ID_{50} of dithiocarbamates compared to xanthates, respectively. Nevertheless, the hypothesis that either dithiocarbamates or xanthates can influence the cytotoxicity of phosphane-gold(1) was opposed when Jamaluddin et al. (2013) reported that the dithiocarbamates in salt form exhibited IC_{50} above 80 μM compared to the dithiocarbamates as ligand bound to triorganophosphane-gold(1) which exerted IC_{50} ranging from 4.4 to 13.6 μM . Therefore, this pattern can also be implied to our current complexes of **1–3**, which can be concluded that their higher cytotoxicities towards MCF-7 and A2780 cell lines were mostly contributed to the tricyclohexylphosphane ligand linearly bound to gold (1). Furthermore, this is supported by Berner-Price et al. (1990) who reported that the variation of anionic ligand was shown to present little effect in cytotoxicity and this is further supported by Gunatilleke and

Barrios (2006) whom stated that changes of thiolate ligand only has little effect towards the activities compared to variation of its phosphine ligand.

It is well known that cancer constitutes a cell autonomous genetic or epigenetic disease and hence the therapeutic efficacy of any antineoplastic agent will highly rely on their ability to influence the tumor-host interaction leading to a balanced mounting of immune response specific for the malignant cells and its microniche (Zitvogel et al. 2013). Hence, understanding the activation status of key signaling pathways that underlies components that links immune responses specific to tumor cells is highly required. Recently, p53 tumor suppressor as a master regulatory transcription factor (in cell cycle arrest, apoptosis, senescence, and metabolism) has gained much focus due to its vital role in tumor immunology and homeostatic regulation of immune responses (Mendez et al. 2013; Muñoz-Fontela et al. 2016). Here in our study, we have investigated the ability of compounds 1–3 to activate p53 signaling pathway and status of p53 mediated genes that will influence tumor regulation to exert anticancer activity in in vitro MCF-7 breast cancer and A2780 cells ovarian cancer model systems.

To investigate the first possibility on the activation status of p53, we have analyzed the status of thioredoxin reductase (TrxR) activity on MCF-7 cells and A2780 cells upon treatment with 1–3. Tumor suppressor p53 is a redox active transcription factor whose activation is also mediated by oxidative status of thioredoxin (Trx) (Liu et al. 2008) Thioredoxin (Trx) is a dithiol-reducing enzyme that is induced by ROS and/or oxidative Trx modulates/regulates the activity of DNA-binding proteins, including p53, Jun/Fos and NFκB. Our results showed that in both MCF-7 and A2780 cells, the activity of TrxR was highly suppressed to about 40% compared to untreated control cells, denoting the compound 1–3 treatment favors accumulation of oxidized thioredoxin.

Among TrxR inhibitors, gold compounds are very effective, acting at nanomolar levels, probably due to the high affinity of gold towards chalcogenides (group 16 donors including S, Se and Te) which renders the nucleophilic selenolate of reduced TrxR the prime target site of modification by this metal (Gandin et al. 2010). In the current findings, comparable TrxR inhibition was seen on MCF-7 cells treated with 1–3, respectively. Nevertheless, 1 has shown greater TrxR

inhibition towards A2780 cells compared to other compounds of 2 and 3. This interesting finding somehow led us to question the role of mercaptobenzoic acid ligand in this experiment. Priorly, Smyth et al. (2001) reported the polymorphism in 1, which consists of four distinct forms; three with rod motif and one with ‘ball’ motif, during the crystallization. Tiekink (2003) also hypothesized that 2-mercaptobenzoate series bound to triorganophosphinegold(1) exhibited interesting profiles due to its selectivity in the cytotoxic profiles of 2-MBA series Structural wise, we suspected that 2-MBA might probably play a partial role in its TrxR inhibition, compared to its other isomeric compound. According to Varghuese et al. (2011), activity of drug might change abruptly from one polymorph to another, which may cause problem in pharmaceutical industries. In addition, an ideal approach in understanding the structure–property relationship in molecular solids could be provided by the comparison between different polymorphs (Meundaeng et al. 2016). Nevertheless, this can only be confirmed once we conducted the same experiment on the compounds by adding the isomeric mercaptobenzoic ligands alone as controls.

Phosphane-gold(1) compounds can inhibit Trx by binding to the active site cysteines and through the oxidation of Trx(SH)₂ to Trx(SS) (Lima and Rodriguez 2011). TrxR is endowed with a flexible C-terminal extension containing a cysteine/selenocysteine redox center that can easily interact with different and chemically unrelated substrates and inhibitors (Nishinaka et al. 2001). In a study reported by Fricker (2010), the ability of the gold(1) compound to inhibit TrxR activity is due to its thiol-containing molecules, which may suggest that the role of thiolate ligand in this experiment. Thiol-containing molecular targets include the redox enzymes thioredoxin reductase and glutathione reductase, transcription factors, and cysteine proteases such as caspases and cathepsins (Fricker 2010). Thiolates are known to act as “soft” ligands forming covalent bonds with the ‘soft’ gold (1) ion; corresponding selenolates are “softer” donor ligands compared to thiolates and, consequently, behave as better substrates for the gold(I) ion (Chaudière and Tappel 1984). Therefore, apart from the MBA and phosphine ligands, the presence of thiolate in our synthesized compounds should have also been taken into account for its effect in inhibiting/suppressing TrxR.

In a recent study by Walther et al. (2020) on carbene-gold(1) thiolate compounds, bound to dithiocarbamate and D-glucopyranosyl, NHC*-AuSCSNMe₂ and NHC*Au-S-GLUC exhibited significant TrxR IC₅₀ of 1.2 ± 0.2 and 7.4 ± 0.4 μ M, respectively. This indicated that the same GLUC ligand in this compound, which also consists in auranofin did not contribute much to the TrxR inhibition activities. Marzo et al. (2020) supported the findings by comparing the TrxR inhibition activity of Auranofin, Et₃PAuCl and Et₃PAuI, respectively, to yield with comparable IC₅₀ of Auranofin and Et₃-PAuCl, but lower IC₅₀ of Et₃PAuCl, yet all the IC₅₀ values were still fell in the nanomolar range.

In addition, the cellular TrxR is in mitochondria plays role in transcription factors for proliferation and apoptosis inhibition and is found to be over expressed in breast, ovarian and colorectal tumors favoring drug resistance (Sasada et al. 1996; Yokomizo et al. 1995; Bhatia et al. 2016). In our study, reduced TrxR activity upon treatment with **1–3** denotes that they regulate cellular proliferation probably by modulating p53 activation and these compounds might directly interact with mitochondria leading to ROS generation (Muniyappa and Das 2008) and thereby inhibiting TrxR activity which is also reported for similar gold nanoparticles (Karataş et al. 2009) and other gold(1) analogues (Walther et al. 2020; Marzo et al. 2020).

Activation of p53 mediates transcription of array of genes that regulates cell cycle arrest, apoptosis, or DNA repair contextually depending upon cell type and stress. Here in our study we performed qPCR analysis in MCF-7 cells and A2780 cells upon treatment with **1–3** compounds to understand the role of p53 activation and their underlying mechanisms of action in exerting antiproliferative action. In MCF-7 cells, we observed up-regulation of *TP53*, *TP53AIP1*, *TP53BP2*, *TP73*, *BAX*, *APAF1*, and *TNF* respectively, whilst *MDM2*, *BCL2*, *NFKB1*, *CDC25A* and *CDC25C* that regulate cell cycle activation, *PCNA* proliferative marker and *RB1* (senescence associated) were down-regulated. Cumulatively, this denotes the test compounds probably cause significant genome damage favoring cell death via apoptosis and with concurrent down-regulation of cell cycle regulators and activates genes promoting cell death, notably *TP53*, *TP53AIP1*, *TP53BP2* and immune regulation *BRCA1*, *BRCA2* etc., (Muñoz-Fontela et al. 2016).

On the other hand, in an ovarian cancer in vitro model, A2780 cells upon treatment of **1–3**, we observed upregulation of *TP53*, *TP53AIP1*, *TP53BP2*, *TP73*, *E2F1*, *APAF1*, *CASP9* that favor apoptosis respectively, whilst *HK2*, *BCL-2*, *CDK-1*, and *CDK-4* which regulate anti-cancer activity and *PCNA* proliferative marker were down-regulated and notably, *RB1* (senescence associated) gene was up-regulated. These may indicate that the gold compounds caused significant oxidative damage by favoring cell death via apoptosis partially and caused induction of senescence associated phenotype in partial (Qian and Chen 2010; Rufini et al. 2013). These are evident from the downregulation of anticancer genes in A2780 cells which is distinct from MCF-7 cells. Our results signified that all compounds exerted antiproliferative activities in both MCF-7 and A2780 cells which may be differed in terms of their mechanisms between both cancer cells.

Polyubiquitination usually occurs at Lys⁴⁸ and Lys⁶³ of ubiquitin. It has been well recognized that while Lys⁴⁸-linked polyubiquitination serves as a universal recognition signal that targets proteins for proteasomal degradation, Lys⁶³-linked polyubiquitination acts primarily as regulatory rather than proteolytic signal (Nathan et al. 2013; Swatek and Komander 2016). The role of p53 as a transcription factor is highly achieved by regulating its protein synthesis and degradation to maintain constant nuclear concentration (Jain and Barton 2010). At the fulcrum of this balance, an array of proteins ligates ubiquitin to lysine residues of target proteins in order to achieve post translational modification (PTM) and to regulate its stability. Hammond-Martel et al. (2012) reported that p53 interacts with array of E3s that targets p53 for self-destruction; however, p53 also interacts with distinct set of E3s that mediates its nuclear localization and stability. For instance, E4F1, an atypical E3 promotes p53-dependent growth arrest probably via activating cell cycle arrest genes, via ubiquitin lysine 48 chain linkages (Cam et al. 2006). In addition, another class of ubiquitin lysine E3 favors monomeric p53 degradation, thereby preventing its multimerization required for its transcription activity (Laine et al. 2006). Thus, we determined the context of p53 functioning upon treatment with **1–3** in the present study. We analysed the status of ubiquitin activities by measuring the levels of Lys48-linked polyubiquitin and Lys63-linked polyubiquitin in MCF-7 and A2780

cancer cells respectively. Our results showed levels of Lys48-linked polyubiquitin was about 92.73%, 89.60% and 90.26%, whilst the activities of Lys63-linked polyubiquitination was found to be about 6.20%, 20.96% and 30.42%. Similarly, in the A2780 cells, the levels of Lys48-linked polyubiquitin was 96.72%, 98.98%, 98.74%, while Lys-63 activities was about 31.10%, 40.60%, 9.74% respectively. Our results depicted that the test compounds increased the activities of ubiquitin Lys-48 whilst simultaneously suppressed Lys-63 in promoting p53 to interact with chromatin, which led to transcriptional initiation of cell cycle arrest genes thereby augmented growth arrest. This postulates that **1–3** exerted potent antiproliferative activities probably via activating and maintaining p53 function as well as preventing its nuclear export and destabilization (Topisirovic et al. 2009; Brooks and Gu 2011; Thiery 2002).

In support to our findings that the compounds **1–3** mediated cell cycle arrest and inhibited tumor growth by activating p53, we performed cell invasion assay on MCF-7 and A2780 cells, respectively. Herein, we observed that both MCF-7 and A2780 cells exhibited significant reduction of cell migration which was more pronounced on MCF-7 cells ($9.29\% \pm 0.2$, $7.41\% \pm 0.28$ and $8.45\% \pm 0.24$), as compared to A2780 cells ($41.5\% \pm 1.4$, $33.86\% \pm 1.24$ and $30.78\% \pm 7.67$). The observed difference in reduced inhibitory cell invasion in A2780 cells could be due to the increased expression of senescent associated genes manifested by the compounds, accompanied by the reduced expression of genes that regulate antiproliferative activity, as priorly discussed. These compounds can alter/regulate the processes of epithelial mesenchymal transition (EMT) on MCF-7 and A2780 cells, which is crucial for cell migration and tumor progression (Schaeffer et al. 2014). Furthermore, the activation of p53 in our study may also favor inhibition of EMT probably by inhibiting NF κ B activation, evidently manifested from reduced activity of ubiquitin Lys63 in our study which is required for NF κ B activation. Notably, these data were also supported by Sui et al. (2015) who evidently documented the inhibition of cancer cell invasion by wild type 53 via suppression of NF κ B mediated activation of fascin, a cytoskeletal protein, whilst p53 deletion augmented cell invasion.

Conclusion

Taken all the findings together, candidate gold compounds **1–3** could activate p53 by modulating p53 target genes expressions, which in turn inhibited cell cycle progression, cytoskeletal reorganization and tumor invasion on the respected MCF-7 and A2780 cells. The observed antiproliferative efficacy of the compounds and their ability to induce p53 activation can be directly associated to their ability to induce oxidative stress via ROS generation, evidently shown from reduced TrxR activity in both in vitro models. Hence, these gold derived drug complexes **1–3** may have potential to further develop as a better therapeutic agent for cancer therapies.

Acknowledgements This research was funded by Ministry of Higher Education, Malaysia, Grant Numbers UM.C/HIR-MOHE/SC/03 and UM.C/HIR-MOHE/SC/12. We thanked Universiti Malaya for providing the grants under High Impact Research Schemes and collaborated with us by providing the compounds and the funding. We also thanked Prof Dr Noor Saadah Abd Rahman, the Deputy Vice Chancellor (Research and Innovation) at the University of Malaya for giving us the consent to publish the data

Author contributions Conceptualization, RAH; methodology, RAH; validation, AKP, CPF and RAH; formal analysis, AKP and CPF; investigation, AKP and CPF; data curation, AKP; writing—original draft preparation, AKP; writing—review and editing, RAH; visualization, AKP and CPF; supervision, RAH; project administration, RAH. All authors have read and agreed to the published version of the manuscript.

Compliance with ethical standards

Conflict of interest The authors declared no conflict of interest.

References

- Almutlaq BA, Almuazzi RF, Almuhayfir AA, Alfouzan AM, Alshammari BT, AlAnzi HF, Ahmed HG (2017) Breast cancer in Saudi Arabia and its possible risk factors. *J Cancer Policy* 12:83–89
- Berners-Price SJ, Girard GR, Hill DT, Sutton BM, Jarrett PS, Faucette LF, Johnson RK, Mirabelli CK, Sadler PJ (1990) Cytotoxicity and antitumor activity of some tetrahedral bis(diphosphino)gold(I) chelates. *J Med Chem* 33:1386–1392
- Bhatia M, McGrath KL, Di Trapani G, Charoentong P, Shah F, King MM, Clarke FM, Tonissen KF (2016) The

- thioredoxin system in breast cancer cell invasion and migration. *Redox Biol* 8:68–78
- Boulikas T, Vougiouka M (2003) Cisplatin and platinum drugs at themolecular level. *Oncol Rep* 10:1663–1682
- Brezden CB, Phillips KA, Abdollell M, Bunston T, Tannock IF (2000) Cognitive function in breast cancer patients receiving adjuvant chemotherapy. *J Clin Oncol* 18:2695–2701
- Brooks CL, Gu W (2011) p53 regulation by ubiquitin. *FEBS Lett* 585:2803–2809
- Chaudière J, Tappel AL (1984) Interaction of gold(I) with the active site of selenium-glutathione peroxidase. *J Inorg Biochem* 20:313–325
- Cookson PD, Tiekink ERT (1992) Syntheses and structural studies of triorganophosphinegold(I) mercaptobenzoate complexes. *J Coord Chem* 26:313–320
- Daigle DJ, Pepperman AB Jr, Vail SL (1974) Synthesis of a monophosphorus analog of hexamethylenetetramine. *J Heterocyclic Chem* 11:407
- Darensbourg DJ, Ortiz CG, Kamplain JW (2004) A new water-soluble phosphine derived from 1,3,5-triaza-7-phosphaadamantane (PTA), † 3,7-diacetyl-1,3,7-triaza-5-phosphabicyclo[3.3.1]nonane. Structural, bonding, and solubility properties. *Organometallics* 23:1747
- de Vos D, Clements P, Pyke SM, Smyth DR, Tiekink ERT (1999) Characterisation and in vitro cytotoxicity of triorganophosphinegold(I) 2-mercaptobenzoate complexes. *Met Based Drugs* 8:303–306
- de Vos D, Smyth DR, Tiekink ER (2002) Cytotoxicity of triorganophosphinegold(I) n-mercaptobenzoates, n = 2, 3 and 4. *Met-Based Drugs* 8:303–306
- de Vos D, Ho SY, Tiekink ER (2004) Cytotoxicity profiles for a series of triorganophosphinegold(I) dithiocarbamates and triorganophosphinegold(I) xanthates. *Bioinorg Chem Appl* 2:141–154
- Donzelli E, Carfi M, Miloso M, Strada A, Galbiati A, Bayssas M, Griffon-Etienne G, Caveletti G (2004) Neurotoxicity of platinum compounds: comparison of the effects of cisplatin and oxaliplatin on the human neuroblastoma cell line SH-SY5Y. *J Neurooncol* 67:65–73
- Elie BT, Levine C, Ubarretxena-Belandia I, Varela-Ramírez A, Aguilera RJ, Ovalle R, Contel M (2009) Water soluble phosphane-gold(I) complexes. Applications as recyclable catalysts in a three-component coupling reaction and as antimicrobial and anticancer agents. *Eur J Inorg Chem* 23:3421–3430
- Ferlay J, Soerjomataram I, Dikshit R, Eser S, Mathers C, Rebelo M, Parkin DM, Forman D, Bray F (2015) Cancer incidence and mortality worldwide: sources, methods and major patterns in GLOBOCAN 2012. *Int J Cancer* 136:E359–E386
- Fricker SP (2010) Cysteine proteases as targets for metal-based drugs. *Metallomics* 2:366–377
- Gandin V, Fernandes AP, Rigobello MP, Dani B, Sorrentino F, Tisato F, Bjornstedt M, Bindoli A, Sturaro A, Rella R, Marzano C (2010) Cancer cell: death induced by phosphine gold(I) compounds targeting thioredoxin reductase. *Biochem Pharmacol* 15:90–101
- Gunatilleke SS, Barrios AM (2006) Inhibition of lysosomal cysteine proteases by a series of Au(I) complexes: a detailed mechanistic investigation. *J Med Chem* 49:3933–3937
- Hammond-Martel I, Yu H, Affar B (2012) Roles of ubiquitin signaling in transcription regulation. *Cell Signal* 24:410–421
- Harris S, Levine AJ (2005) The p53 pathway: positive and negative feedback loops. *Oncogene* 24:2899–2908
- Jain AK, Barton MC (2010) Making sense of ubiquitin ligases that regulate p53. *Cancer Biol Ther* 10:665–672
- Jamaludin NS, Goh ZJ, Cheah YK, Ang KP, Sim JH, Khoo CH, Fairuz ZA et al (2013) Phosphane-gold(I) dithiocarbamates, R3PAu[SC(=S)N(i)Pr]CH2CH2OH] for R = Ph, Cy and Et: role of phosphane-bound R substituents upon in vitro cytotoxicity against MCF-7R breast cancer cells and cell death pathways. *Eur J Med Chem* 67:127–141
- Jin S, Levine AJ (2001) The p53 functional circuit. *J Cell Sci* 114:4139–4140
- Karataş OF, Sezgin E, Aydin O, Culha M (2009) Interaction of gold nanoparticles with mitochondria. *Colloids Surf B* 71:315–318
- Laine A, Topisirovic I, Zhai D, Reed JC, Borden KL, Ronai Z (2006) Regulation of p53 localization and activity by Ubc13. *Mol Cell Biol* 26:8901–8913
- Le Cam L, Linares K, Paul C, Julien E, Lacroix M, Hatchi E, Triboulet R, Bossis G, Shmueli A, Rodriguez MS, Coux O, Sardet C (2006) E4F1 is an atypical ubiquitin ligase that modulates p53 effector functions independently of degradation. *Cell* 127:775–788
- Lima JC, Rodriguez L (2011) Phosphine-gold(I) compounds as anticancer agents: general description and mechanisms of action. *Anticancer Agents Med Chem* 11:921–928
- Liu B, Chen Y, St. Clair DK (2008) ROS and p53: versatile partnership. *Free Radic Biol Med* 44:1529–1535
- Marzo T, Cirri D, Gabbiani C, Gamberi T, Magherini F, Messori L et al (2020) Auranofin, Et3PAuCl, and Et3PAuI are highly cytotoxic on colorectal cancer cells: a chemical and biological study. *ACS Med Chem Lett* 8:997–1001
- Menendez D, Shatz M, Resnick MA (2013) Interactions between the tumor suppressor p53 and immune responses. *Curr Opin Oncol* 25:85–92
- Meundaeng N, Rujiwatra A, Prior TJ (2016) Polymorphism in metal complexes of thiazole-4-carboxylic acid. *Transit Met Chem* 41:783–793
- Mosmann T (1983) Rapid colorimetric assay for cellular growth and survival: application to proliferation and cytotoxicity assays. *J Immunol Methods* 65:55–63
- Muniyappa H, Das KC (2008) Activation of c-Jun N-terminal kinase (JNK) by widely used specific p38 MAPK inhibitor SB202190 and SB203580: A MLK-3-MKK7-dependent mechanism. *Cell Signal* 20:675–683
- Muñoz-Fontela C, Mandinova A, Aaronson SA, Lee SW (2016) Emerging roles of p53 and other tumour-suppressor genes in immune regulation. *Nat Rev Immunol* 16:741–750
- Nathan JA, Kim HT, Ting L, Gygi SP, Goldberg AL (2013) Why do cellular proteins linked to K63-polyubiquitin chains not associate with proteasomes? *EMBO J* 32:552–565
- Nishinaka Y, Nakamura H, Masutani H, Yodoi J (2001) Redox control of cellular function by thioredoxin: a new therapeutic direction in host defense. *Arch Immunol Ther Exp* 49:285–292

- Qian Y, Chen X (2010) Tumor suppression by p53: making cells senescent. *Histol Histopathol* 25:515–526
- Rufini A, Tucci P, Celardo I, Melino G (2013) Senescence and aging: the critical roles of p53. *Oncogene* 32:5129–5143
- Sasada T, Sono H, Yodoi J (1996) Thioredoxin/adult T-cell leukemia-derived factor (ADF) and redox regulation. *J Toxicol Sci* 21:285–287
- Schaeffer D, Somarelli JA, Hanna G, Palmer GM, Garcia-Blanco MA (2014) Cellular migration and invasion uncoupled: increased migration is not an inexorable consequence of epithelial-to-mesenchymal transition. *Mol Cell Biol* 34:3486–3499
- Selenius M, Hedman M, Brodin D, Gandin V, Rigobello MP, Flygare J, Fernandes AP et al (2012) Effects of redox modulation by inhibition of thioredoxin reductase on radiosensitivity and gene expression. *J Cell Mol Med* 16:1593–1605
- Sharma HK, Chhangte L, Dolui AK (2001) Traditional medicinal plants in Mizoram, India. *Fitoterapia* 72:146–161
- Smyth DR, Vincent BR, Tiekink ERT (2001) Polymorphism in (tricyclohexylphosphine)gold(I) 2-mercaptobenzoate. a tale of two structural motifs. *Crystal Growth Design* 1:113–117
- Stegh AH (2012) Targeting the p53 signaling pathway in cancer therapy - the promises, challenges and perils. *Exp Opin Ther Targets* 16:67–83. <https://doi.org/10.1517/14728222.2011.643299>
- Sui X, Zhu J, Tang H, Wang C, Zhou J, Han W, Wang X, Fang Y, Xu Y, Li D, Chen R, Ma J, Jing Z, Gu X, Pan H, He C (2015) p53 controls colorectal cancer cell invasion by inhibiting the NF- κ B-mediated activation of Fascin. *Oncotarget* 6:22869–22879
- Swatek KN, Komander D (2016) Ubiquitin modifications. *Cell Res* 26:399–422
- Taguchi T, Nazneen A, Abid MR, Razzaque MS (2005) Cisplatin associated nephrotoxicity and pathological events. *Contrib Nephrol* 14:107–121
- Thiery JP (2002) Epithelial-mesenchymal transitions in tumour progression. *Nat Rev Cancer* 2:442–454
- Tiekink ERT (2002) Gold derivatives for the treatment of cancer. *Crit Rev Oncol Hematol* 42:225–248
- Tiekink ERT (2003) Gold compounds in medicine: potential anti-tumour agents. *Gold Bull* 36:117–124
- Topisirovic I, Siddiqui N, Orolicki S, Skrabanek LA, Tremblay M, Hoang T, Borden KLB (2009) Stability of eukaryotic translation initiation factor 4E mRNA is regulated by HuR, and this activity is dysregulated in cancer. *Mol Cell Biol* 29:1152–1162
- Trudu F, Amato F, Vaňhara P, Pivetta T, Peña-Méndez EM, Havel J (2015) Coordination compounds in cancer: past, present and perspectives. *J Appl Biomed* 13:79–103
- Varughese S, Kiran KSRN, Solanko KA, Bond AD, Desiraju GR (2011) Interaction anisotropy and shear instability of aspirin polymorphs established by nanoindentation. *Chem Sci* 2:2236–2242
- Vogelstein B, Lane D, Levine AJ (2000) Surfing the p53 network. *Nature* 408:307–310
- Walther W, Althagafi D, Curran D, O’Beirne C, Mc Carthy C, Ott I, Tacke M et al (2020) In-vitro and in-vivo investigations into the carbene-gold anticancer drug candidates NHC*-Au-SCSNMe2 and NHC*-Au-S-GLUC against advanced prostate cancer PC3. *Anticancer Drugs* 31:672–683
- Wetzel C, Kunz PC, Kassack MU, Hamacher A, Böhler P, Watjen W, Ott I, Rubbiani R, Spingler B (2011) Gold(I) complexes of water-soluble diphos-type ligands: synthesis, anticancer activity, apoptosis and thioredoxin reductase inhibition. *Dalton Trans* 40:9212–9220
- Yokomizo A, Ono M, Nanri H, Makino Y, Ohga T, Wada M (1995) Cellular levels of thioredoxin associated with drug sensitivity to cisplatin, mitomycin C, doxorubicin and etoposide. *Cancer Res* 55:4293–4296
- Zitvogel L, Galluzzi L, Smyth MJ, Kroemer G (2013) Mechanism of action of conventional and targeted anticancer therapies: reinstating immunosurveillance. *Immunity* 39:74–88

Publisher’s Note Springer Nature remains neutral with regard to jurisdictional claims in published maps and institutional affiliations.